Development of nanoscale polarization fluctuations in relaxor-based (1-x)Pb(Zn1/3Nb2/3)03-xPbTi03 ferroelectrics studied by Brillouin scattering

Development of nanoscale polarization fluctuations in relaxor-based (1-x)Pb($Zn_{1/3}Nb_{2/3}$)O_3-$x$$PbTiO_3$ ferroelectrics studied by Brillouin scattering

Shinya Tsukada*
Pure and Applied Sciences, University of Tsukuba, Tsukuba City, Ibaraki 305-8573, Japan and
Faculty of Education, Shimane University, Matsue City, Shimane 609-8504, Japan

Yuki Hidaka and Seiji Kojima†
Pure and Applied Sciences, University of Tsukuba, Tsukuba City, Ibaraki 305-8573, Japan

Alexei A. Bokov and Zuo-Guang Ye‡
Department of Chemistry and 4D LABS, Simon Fraser University, Burnaby, British Columbia, V5A 1S6, Canada
(Received 2 July 2012; revised manuscript received 3 December 2012; published 2 January 2013)

The precursor dynamics of ferroelectric phase transitions in relaxor-based ferroelectric $(1-x)$ Pb($Zn_{1/3}Nb_{2/3}$)O_3-$x$$PbTiO_3$ single crystals, with $x = 0.07$, 0.10, and 0.12, were investigated using inelastic light scattering from a longitudinal acoustic phonon. An acoustic anomaly in a broad temperature range, which is characteristic of relaxor ferroelectrics, was observed. We describe the anomalies in the paraelectric phase by assuming local piezoelectric coupling inside polar nanoregions, which are surrounded by a nonpolar matrix. On the basis of local piezoelectric coupling, a relaxation time τ and a dynamic characteristic length L of the order-parameter (polarization) fluctuations were determined to be in the order of 10^{-13} s and 10^{-9} m, respectively. The τ and L values increase sharply upon cooling from high temperatures but more gradually below the intermediate temperature T^* (=493 − 510 K). This result implies that the local polarization fluctuations grow rapidly upon cooling down to above T^* and the growth rate decreases below T^*. The inflexion point of this growth process in the paraelectric phase is related to the characteristic properties of relaxor-based solid solutions.

DOI: 10.1103/PhysRevB.87.014101 PACS number(s): 77.80.Jk, 78.35.+c

I. INTRODUCTION

The phenomena of inhomogeneous systems have attracted a great deal of research in the field of condensed matter science. Intrinsic inhomogeneity in complex oxides induces a few kinds of unusual behavior. For example, microtwins—inhomogeneity in shape-memory alloys—induce recoverable giant strain,[1] while nanometer-sized conductive regions in manganite induce colossal magnetoresistance.[2] In the case of relaxor ferroelectrics, local polar regions of several nanometers wide, called polar nanoregions (PNRs), are believed to contribute to giant dielectric and electromechanical responses.[3] These properties find a wide range of technological applications; however, their microscopic mechanisms, especially the effects of inhomogeneity on macroscopic phenomena, such as the ferroelectric phase transition in relaxor ferroelectrics, remain poorly understood.

Relaxor behavior is found in various kinds of compounds, for instance, Pb(B′B″)O_3-$PbTiO_3$, ($Sr_{1-x}Ba_x$)Nb_2O_6, and (K_3Li_{2-x})$Nb_{5+x}O_{15+2x}$. In particular, the single crystals of perovskite relaxor-based ferroelectric Pb(B′B″)O_3-$PbTiO_3$ solid solutions possess extremely high dielectric, piezoelectric, and electrostrictive properties, making them the materials of choice for the next generation of electromechanical devices for sensing and actuation.[4]

Relaxor ferroelectrics are distinguished from normal ferroelectrics by the broad and frequency-dispersive maximum in the temperature dependence of the dielectric constant. From a structural point of view, the inhomogeneous arrangement of different ions on crystallographically equivalent sites is another common feature of relaxor ferroelectrics. It is believed that the disorder, due to the different ions at equivalent lattice sites, generates PNRs at much higher temperatures than a ferroelectric phase-transition temperature, leading to relaxor phenomena. Since PNRs are directly responsible for the various properties, the study of the dynamics of PNRs is essential for a better understanding of the intricate phase transitions in relaxor ferroelectrics.[3]

The phase transitions and PNR behavior in relaxor ferroelectrics can be described using four characteristic temperatures. From the highest to the lowest, these are (i) the Burns temperature T_B,[5] (ii) the intermediate temperature T^*,[6–8] (iii) the frequency-dependent temperature of the dielectric permittivity peak T_m, and (iv) the ferroelectric phase transition temperature T_C [or the freezing temperature T_f in the case in which this transition is absent as, e.g., in Pb($Mg_{1/3}Nb_{2/3}$)O_3 (PMN)].[9] Above T_B, the phase is paraelectric without PNRs, and the structure is essentially the same as the paraelectric state of normal ferroelectrics. Below T_B, in the so-called ergodic relaxor phase, the frustration between electric and spatial instabilities induces PNRs, despite the fact that the macroscopic crystal symmetry is identical to that above T_B. In this temperature range, the dynamics of PNRs affects the macroscopic properties. For example, the refractive index deviates from the linear temperature dependence below T_B.[5] Another example is that the temperature dependence of the dielectric constant does not obey the Curie-Weiss law.[10] Between T_B and T^*, it is thought that the fluctuating PNRs are dispersed. Below T^*, the static components of PNRs start to appear, leading to a change in the Raman spectra and a deviation from the linear temperature dependence of expansion coefficient.[6,11] When dynamic PNRs transform into static

PNRs, an acoustic emission (AE) burst is observed at T^*.[7,8] The polarization fluctuations increase toward T_m. At this time, the polarization fluctuations are composed of both dynamic PNRs and polar fluctuations at the static PNR boundaries. Then, the static PNRs become larger and can correlate to each other strongly enough to form macroscopic ferroelectric domains at T_C. Note that even at low temperatures, PNRs exist, and their interactions contribute to ferroelectric responses.[12,13]

Due to the presence of PNRs, peculiar properties are observed in relaxor ferroelectrics. As mentioned above, the alignment of PNRs induces ferroelectric ordering; therefore, the fluctuations related with the alignment in the paraelectric phase should be an important phenomenon to investigate.[12,13] The polarization dynamics in relaxor ferroelectrics is so complicated that it needs to be studied from diverse viewpoints. Thus, dielectric measurement, inelastic light scattering (both Brillouin and Raman scatterings), inelastic neutron scattering, and inelastic x-ray scattering have been performed in various studies.[11,14–23]

Of note, the study of acoustic phonons in ferroelectric materials is one of the most powerful approaches for investigating the polarization fluctuations related to a ferroelectric phase transition.[24] This is because acoustic properties are influenced by polarization fluctuations through strain-polarization coupling. In the present study, we have probed the acoustic phonons in relaxor-based ferroelectric $(1-x)$ $Pb(Zn_{1/3}Nb_{2/3})O_3$-$x$$PbTiO_3$ (PZN-xPT) crystals (with $x =$ 0.07, 0.10, and 0.12) by measuring inelastic light scattering in the gigahertz range (i.e., the Brillouin scattering). Here, the phase diagram, T^*, and T_B were already reported in Refs. 7,8, and 25. The solid solution of PZN-xPT exhibits interesting phase behavior, with the rhombohedral symmetry on the PZN-rich side ($x < 0.08$) at room temperature, transforming into the tetragonal phase with increasing PT concentration ($x > 0.11$). A morphotropic phase boundary (MPB) is formed in the composition range of $0.08 < x < 0.11$, where a lower-symmetry (orthorhombic) phase exists.[26] By investigating the temperature dependence of acoustic phonons of three PZN-xPT compositions, we have examined the behavior of PNRs at the ferroelectric phase transitions in these relaxor-based ferroelectrics. In our previous study, the relaxation observed at the central peak was related to the acoustic anomalies observed in PZN-0.07PT.[20] A comprehensive explanation of the acoustic anomalies of relaxor ferroelectrics is presented in this paper, which is based on the determination of the relaxation times of polarization fluctuations that couple to the strain fluctuations in the PZN-xPT crystals. The dynamic correlation length of the relaxation time is also discussed.

II. EXPERIMENTS

Single crystals of PZN-0.07PT were grown using the high-temperature flux technique with PbO-based fluxes (Microfine Materials Technologies),[27] while PZN-0.10PT and PZN-0.12PT single crystals were grown using the top-cooled solution growth technique.[28] Platelets of pseudocubic (100) orientation were cut from the as-grown crystals for the subsequent experiments.

An acoustic phonon at $|\boldsymbol{k}| \approx 0$ was observed through inelastic light scattering. The light scattering was measured with a high-contrast $3+3$-pass tandem Fabry-Perot interferometer (JRS Scientific Instruments) combined with an optical microscope (Olympus). A diode-pumped solid-state laser (Coherent Inc.) with a single-frequency operation at 532 nm at 100 mW was used. A 180° scattering geometry without a polarizer (vertical to open) was adopted for observing the LA phonon. In this scattering geometry, only the LA phonon along the $[100]_C$ direction was observed in the cubic phase. For temperature variation between 80 and 873 K, the sample was placed inside a cryostat cell (Linkam), and measurements were performed upon cooling for PZN-xPT ($x = 0.07, 0.12$) and upon heating for PZN-0.10PT. Because the LA phonon of relaxor ferroelectrics behaves in the same manner above T_C, there is no difference between the measurements on cooling and on heating.

The complex dielectric constant ($\varepsilon^* = \varepsilon' - j\varepsilon''$) of a PZN-0.07PT single crystal was measured using an LCR meter (Solartron) in the $[100]_C$ direction. The measurements were performed upon cooling at a rate of 1 K min^{-1}. The temperature was controlled by a homemade furnace. Ag paste was painted on each of the parallel plane (100) faces of a crystal as electrodes.

III. RESULTS AND DISCUSSION

Figure 1 shows the contour map of the inelastic light scattering intensity of PZN-0.07PT as a function of frequency shift and temperature under the geometry of 180° scattering

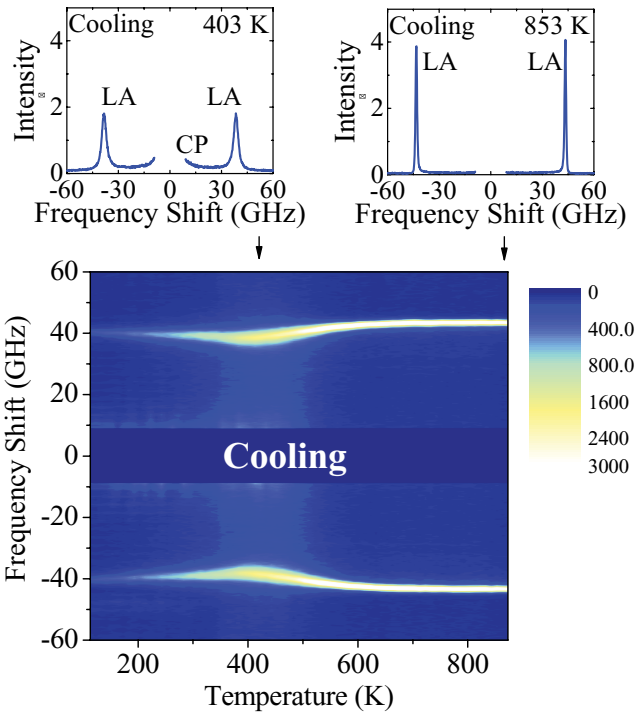

FIG. 1. (Color online) Contour map of inelastic light scattering intensity from PZN-0.07PT crystal versus temperature and frequency shift in $x(zy+z)\bar{x}$ scattering geometry (FSR = 75 GHz, scan range = 70.5 GHz). The temperature-dependent inelastic scattering from the LA phonon is clearly observed. The dark parts at 0 GHz denote elastic scattering. The scattering was measured upon cooling without a polarizer. Note that 1 [meV] = 242 [GHz].

$x(z\,y+z)\bar{x}$, where x, y, and z denote the cubic axes. The spectrum consists of an LA phonon at ± 42 GHz and a central peak at 0 GHz. The transverse-acoustic phonons do not appear due to the symmetry restriction of the cubic photoelastic tensor. In PZN-0.07PT, the average crystal structure transforms from ferroelectric rhombohedral to ferroelectric tetragonal at 390 K, then to paraelectric cubic at 420 K($= T_C$) upon heating.[25] The characteristic temperatures of PNRs in PZN-0.07PT are also known: $T_B \approx 736$ K and $T^* \approx 499$ K.[8]

Figure 1 shows a clear anomaly in the LA phonon at around 390 K; the LA phonon softens when approaching T_C on the cooling run, while at the same time, the peak broadens. Because the phase transitions are smeared by the fine domain structure on the cooling measurement,[29] only one minimum was observed in PZN-0.07PT. The anomalous temperature dependence of the LA phonon is typical of the ferroelectric phase transitions in perovskite ferroelectrics through the strain-polarization coupling in the free energy. However, the temperature range is especially wide around the phonon anomaly in PZN-0.07PT, reflecting the characteristics of relaxor ferroelectrics. In addition to the LA phonon, a central peak is observed in a broad frequency range, which increases in intensity with decreasing temperature and becomes strongest around T_C. This peak is also a characteristic of relaxor ferroelectrics, and its interpretation was discussed in our previous works.[17,19,20,22]

To extract the frequency shift and width of the LA phonon from the light scattering spectra, we used the Voigt function. The width of a Gaussian component in the Voigt function was fixed as an instrumental function. The computed parameters of the acoustic phonons, including Brillouin shift ν_B and full width at half-maximum (FWHM) Γ, are shown in Fig. 2 as a function of temperature for the three PZN-xPT crystals ($x = 0.07, 0.10$, and 0.12). The figure shows two characteristic temperatures, T_B and T_C. Below $T_B \sim 740$ K, ν_B deviates from a linear temperature dependence markedly, which is attributed to the appearance of PNRs below this temperature. That is, the PNRs induce additional polarization fluctuations, and this simultaneously generates strain fluctuations through polarization-strain coupling. In Fig. 2, ν_B and Γ show a minimum and a maximum at T_C, respectively, for each of the crystals, indicating that the dynamic polarization fluctuations at T_C are the greatest of all temperatures. The acoustic anomaly at T_C becomes sharper as x increases in the PZN-xPT crystals, showing that the ferroelectric phase transition from paraelectric cubic phase to ferroelectric tetragonal phase tends to be a normal one. The temperature dependence of the dielectric constant of PZN-0.07PT is shown in Fig. 3, where a jump is found in both ε' and ε'' at 390 K, which corresponds to the T_C observed in the LA phonon in Fig. 2. ν_B and Γ are related to the sound velocity V, an absorption coefficient α, and the complex elastic stiffness constant $c_{11}^* = c_{11}' - jc_{11}''$ through the equations

$$V = \sqrt{\frac{c'(\omega_s)}{\rho}} = \frac{2n\sin(\theta/2)}{\lambda_0}\nu_B, \tag{1}$$

$$\alpha = \frac{\omega_s}{2\rho V^3}c''(\omega_s) = \frac{\pi\Gamma}{V}, \tag{2}$$

where, ρ denotes the density, θ is the scattering angle, λ_0 is the wavelength of the incident beam, n denotes the refractive index, and ω_s is the angular frequency of the acoustic phonon connected with ν_B, $\omega_s = 2\pi\nu_B$.

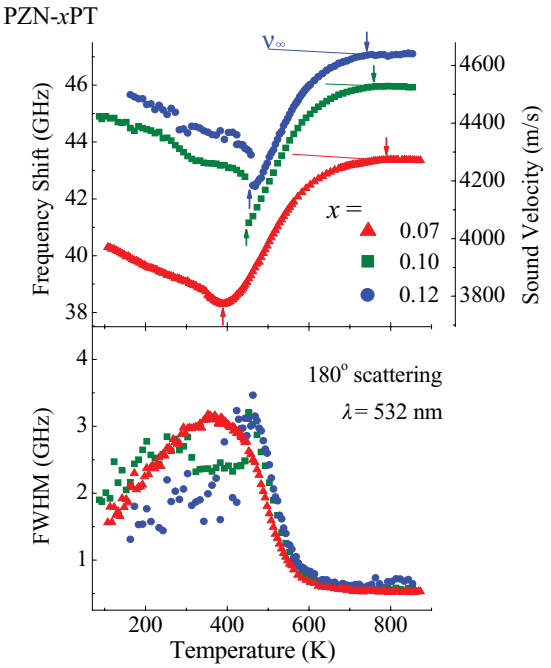

FIG. 2. (Color online) Frequency shift ν_B and FWHM Γ of Brillouin scattering of PZN-xPT crystal, determined by fitting the spectra. The right axis denotes the hypersound velocity that is calculated by Eq. (1) under $\theta = 180°$, $\lambda_0 = 532 \times 10^{-9}$ m, and $n = 2.7$. The solid lines at high temperature denote the high-frequency limit of the Brillouin shift of each PZN-xPT ν_∞, where ν_B deviates from below T_B. T_C is marked by up-pointing arrows.

A. Elastic anomaly above the Curie temperature

First, we discuss why the anomaly in the LA phonon occurs in a broad temperature range in the paraelectric and ergodic relaxor phases, where ν_B deviates from the usual linear temperature dependence of ν_∞ (that is, ν_B at the

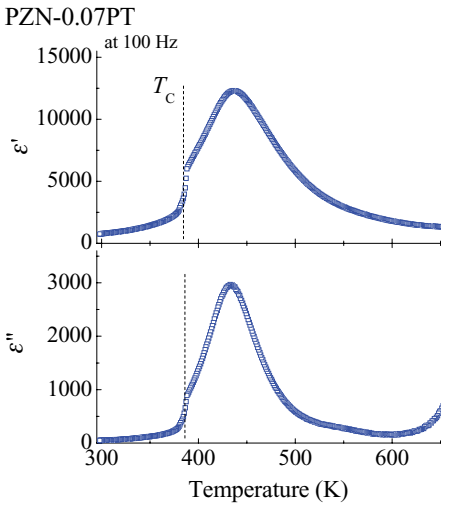

FIG. 3. (Color online) Variations of the real and imaginary parts of the complex dielectric constant ε' and ε'' of PZN-0.07PT crystal as a function of temperature.

high-frequency limit) at far above T_C. The anomalous range in the paraelectric phase is between 390 K ($=T_C$) and 790 K ($=T_B+50$ K) in PZN-0.07PT, between 425 K ($=T_C$) and 760 K ($=T_B+20$ K) in PZN-0.10PT, and between 460 K ($=T_C$) and 740 K ($\sim T_B$) in PZN-0.12PT (as shown in Fig. 2). In the same temperature range, Γ increases upon cooling. The increase of PT content results in sharp anomalies in both ν_B and Γ, reflecting the sharpening of dielectric anomaly at the phase transition with increasing x in PZN-xPT.

The deviation of ν_B from ν_∞ and the increase in Γ above T_C in Fig. 2 indicate the appearance of fluctuations in strain. The increased $\Gamma(\Gamma \propto c''_{mn})$ generally results from energy dissipation that is transferred to thermal fluctuations. For a ferroelectric material, the increase in Γ toward T_C means the growing thermal fluctuations of polarization that is related to the ferroelectric phase transition. The anomalous behavior in the dynamic susceptibility is usually understood using the fluctuation-dissipation theorem (FDT)[24]

$$c''_{mn}(\omega_s) = \frac{\omega_s V}{2k_B T}\int_{-\infty}^{\infty} \exp(i\omega_s t)\langle \delta\sigma_m(t)\delta\sigma_n^*(0)\rangle dt \quad m,n = 1,2\ldots,6, \tag{3}$$

which connects the imaginary part of the susceptibility c''_{mn} with the Fourier transform of the time-correlation function of the internal stress fluctuation $\delta\sigma_m$ in a volume V. Using the Kramers-Kronig transform, the anomaly in c'_{mn} is also described by a time-correlation function. In the present study on ferroelectric phase transition, $\delta\sigma_m$ that is related to the order-parameter fluctuation will be discussed.

Using the proper equation for the free coupling energy F_C, one can express stress fluctuations in terms of the polarization (order parameter) $\langle P\rangle = P_S$ and its fluctuations δP_i. For example, in the case of linear (piezoelectric) coupling, we obtain

$$\delta\sigma_m = \sum_i \beta_{im}\delta P_i \quad i = 1,2,3, \tag{4}$$

where β_{mn} is a coupling constant. Equation (3) is rewritten as

$$c''_{mn}(\omega_s) = \sum_{i,j}\beta_{im}\beta_{jn}\mathrm{Im}\chi_{ij}(\omega_s), \tag{5}$$

using the FDT for the dielectric susceptibility $\chi_{ij} = \chi'_{ij} + i\chi''_{ij}$. Using the Kramers-Kronig transform, the anomalous behavior in the real part is expressed as

$$c'_{mn}(\omega_s) = c'_{mn}(\infty) - \sum_{i,j}\beta_{im}\beta_{jn}\mathrm{Re}\chi_{ij}(\omega_S). \tag{6}$$

In the case of quadratic coupling of the order parameter (electrostrictive coupling), the stress fluctuations are written as

$$\delta\sigma_m = \sum_{i,j}\gamma_{ijm}(\langle P_i\rangle\,\delta P_j + \langle P_j\rangle\delta P_i + \delta P_i\delta P_j) \quad i,j = 1,2,3, \tag{7}$$

and c''_{mn} is expressed by the sum of the linear coupling and a four-point correlation function describing the fluctuation interactions.[24]

Above T_C, typical perovskite ferroelectrics such as $PbTiO_3$ do not show any anomaly in the LA phonon or only show anomalies in a narrow temperature range of less than 10 K wide,[30] because the piezoelectric coupling is prohibited in their paraelectric phases due to the symmetry restriction. In this case, the electrostrictive coupling, as shown in Eq. (7), contributes to the elastic anomaly. Consequently, the elastic anomaly in the paraelectric phase becomes smaller, compared with that of a ferroelectric phase in which piezoelectric coupling is allowed. However, ferroelectric materials with disorder, e.g., relaxor ferroelectrics and barium titanate-($BaTiO_3$-) based ferroelectrics show the anomaly in a much wider temperature range.[17–20,22,31–33] We attribute the anomaly to a piezoelectric coupling inside the noncentrosymmetric disordered regions. Because the local structure inside the PNRs is noncentrosymmetric,[3,12,13] even though the matrix around the PNR is centrosymmetric, the polarization fluctuation can couple linearly with the strain fluctuation. On the assumption of the existence of piezoelectric coupling, we determine the relaxation time of the polarization in Sec. III C.

Slight deviation of ν_B from ν_∞ in a narrow temperature range above T_B is shown in Fig. 2. It is related with the TO phonon condensation. As reported in Refs. 16 and 34, one zone-center TO phonon of relaxor ferroelectrics softens upon cooling toward T_B from above, and such polarization fluctuation can induce the strain fluctuation. In this temperature range, no PNR exists, and consequently, not piezoelectric coupling, but electrostrictive coupling dominates the elastic property. This is why the change in LA phonon above T_B is much smaller than that below T_B.

Recent experimental evidence demonstrates that the ferroelectric phase transition of relaxor ferroelectrics is not a displacive phase transition but is, in fact, an order-disorder-type ferroelectric phase transition,[12,13] in which the fluctuating component must be a relaxation of the PNR. Consequently, considering the fluctuating component inside the noncentrosymmetric PNR using Eq. (5) is a valid approach for simulating the dynamic properties.

B. Elastic anomaly at T^*

In the previous section, we examine the characteristic temperatures of PNRs and point out two anomalies in the acoustic phonon at T_B and T_C, respectively. In addition, an anomaly at T^* is detected, as shown in Fig. 4, which presents the temperature derivative of the LA phonon's width $d\Gamma/dT$. A clear minimum is seen in $d\Gamma/dT$ at 493 K in PZN-0.07PT, 498 K in PZN-0.10PT, and 513 K in PZN-0.12PT. These temperatures are located between T_B and T_C and are in good agreement with the T^* temperature observed in the AE measurements.[7,8] Anomalies in some physical properties around T^* are sometimes regarded as a result of the near-surface effect.[35] However, the anomaly in $d\Gamma/dT$ is found not only in a 180° scattering geometry but also in a 90° scattering geometry, which probes internal crystals. We can therefore conclude that the LA phonon anomaly at T^* is an intrinsic effect.[18–20,22]

We attribute the elastic anomaly in the paraelectric phase to the polarization fluctuation through the piezoelectric coupling. This is described in Eq. (5), in which a large Γ (due to $c'' \propto \Gamma$) indicates a large polarization fluctuation. The derivative $d\Gamma/dT$ represents the inflexion point of Γ, and

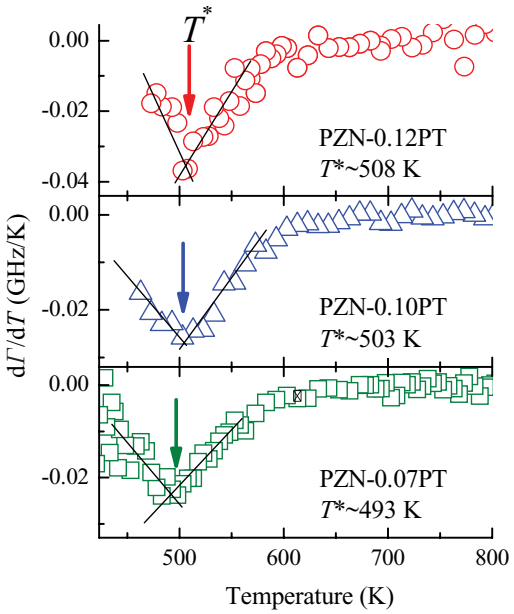

FIG. 4. (Color online) Temperature derivative of the LA phonon's FWHM, $d\Gamma/dT$, of PZN-xPT, with $x = 0.07, 0.10$, and 0.12. $d\Gamma/dT$ shows an extremum at T^*.

Eq. (5) shows that this is induced by the inflexion point of $\chi''_{mn}(\omega_s) = \varepsilon''_{mn}(\omega_s)$, where ω_S is around 40 GHz. From this consideration, $d\Gamma/dT$ can be read as the growth rate of the dynamic polarization fluctuation per kelvin at a frequency of ω_S Hz. Consequently, T^*, at which the minimum in $d\Gamma/dT$ appears, is the changing point: the growth rate increases upon cooling from high temperatures down to T^*, and it decreases below T^*.

Neutron and x-ray diffuse scattering appears clearly in relaxor ferroelectrics.[14,36,37] The diffuse scattering grows and its width markedly decreases below T^*. In addition, the lattice parameter, Raman scattering, and AE show anomalies at T^*.[6–8,11] The piezoelectric force microscopy probes nanodomains below T^*.[38] These are interpreted by the fact that static PNRs start to appear below T^*. On the basis of this interpretation, we reach the following understanding: the appearance of static PNRs below T^* induces a random static electric field, which then suppresses the dynamic polarization fluctuation. Thus, the growth rate of the dynamic polarization fluctuation is reduced below T^*, leading to the appearance of the minima in $d\Gamma/dT$ through piezoelectric coupling.

There are a number of similarities between relaxor ferroelectrics and $BaTiO_3$, both having mesoscopic disorders, and as a result, similar elastic anomalies are observed at T_B and T_C.[5,19,20,31–33,39] From the macroscopic point of view, the difference between them is the appearance of inflexion points in ν_B, Γ, ε', and ε''. For example, Fig. 5 shows that there is no inflexion point in Γ for $BaTiO_3$,[31] as the first derivative of Γ shows no extremum. From the microscopic point of view, we attribute the difference to the growth process of the dynamic polarization fluctuation. In the case of a ferroelectric phase transition in $BaTiO_3$, the growth is never suppressed above T_C, and $d\Gamma/dT$ drops at T_C, as shown in Fig. 5. Thus, the temperature dependence of ε' in $BaTiO_3$ shows a sharp anomaly at T_C. On the other hand, in relaxor ferroelectrics, the

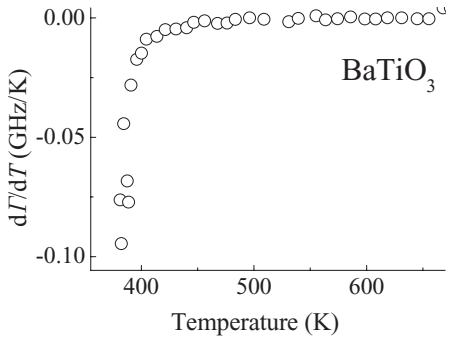

FIG. 5. Temperature derivative of the LA phonon's FWHM $d\Gamma/dT$ of $BaTiO_3$. The data were obtained by reanalyzing the results of Ko *et al.*[31] $d\Gamma/dT$ shows no extremum above T_C.

growth rate decreases at T^*, which leads to the minimum in $d\Gamma/dT$, as shown in Fig. 4. This change in the growth rate at T^* induces the broad peak in ε' at T_m.

C. Polarization relaxation coupled with the LA phonon

If we assume that only one Debye-type dielectric relaxation,

$$\chi^*(\omega_s) = \frac{\chi(0)}{1 - i\omega_s\tau}, \tag{8}$$

is coupled to the LA phonon through the piezoelectric coupling, Eqs. (5) and (6) can be reduced to the Landau-Khalatnikov mechanism written as

$$c'(\omega_s) = c'(\infty) - \frac{c'(\infty) - c'(0)}{1 + (\omega_s\tau)^2}, \tag{9}$$

$$c''(\omega_s) = \frac{\left[c'(\infty) - c'(0)\right]\omega_s\tau}{1 + (\omega_s\tau)^2}, \tag{10}$$

where, τ denotes the relaxation time of the assumed Debye-type relaxation and $c'(0)$ is a constant c' at the low-frequency limit, which is determined by $\chi(0)$ and β_{ij}. From Eqs. (9) and (10) and the relationships between c^* and Brillouin scattering and between V and α [Eqs. (1) and (2)], τ can be simplified as

$$\tau = \frac{\Gamma}{2\pi\left(\nu_\infty^2 - \nu_B^2\right)}. \tag{11}$$

In Eq. (11), Γ and ν_∞ denote the FWHM related to the phase transition and a linear temperature dependence of $\nu_B = A + BT$ much above T_B, respectively. The parameters A and B are determined by the least-squares fitting technique. The resulting values of τ are shown in Fig. 6 for three specimens. As x increases, the rate of change of τ increases, and the relaxation time becomes longer. Interestingly, τ does not go larger than 1×10^{-12} s, and its increase appears to be disturbed below T^*. We note that τ in KF-substituted $BaTiO_3$, determined in the same way, obeys the critical slowing down, i.e., τ becomes larger and larger toward T_C.[31–33] The differences in τ between PZN-xPT and KF-substituted $BaTiO_3$ should reflect the different growing processes of their PNRs, as discussed in Sec. III B. Because the relaxation processes in the gigahertz region are not as complex as in the lower frequencies, we believe that our assumption about the Debye-type relaxation [Eq. (8)] is reasonable.

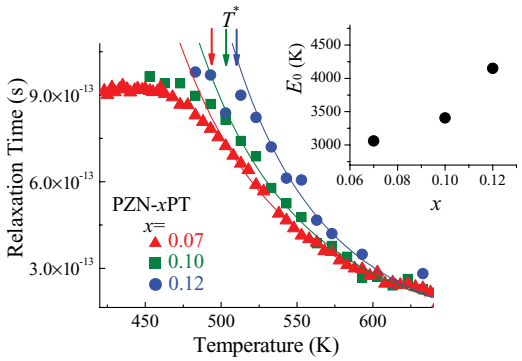

FIG. 6. (Color online) Temperature dependence of the relaxation time of PZN-xPT with $x = 0.07, 0.10$, and 0.12 above T_C. The relaxation times were determined using Eq. (11). The solid lines denote the fitted results by using modified superparaelectric model [Eq. (12)]. The fitted parameters are tabulated in Table I. Inset: x dependence of E_0.

The linear dependence of τ vs $1000/T$ above T^* appears (not shown), suggesting the thermal activation process of the relaxation. It is usual to fit the dependence with the Arrhenius law of $\tau = \tau_0 \exp(E/k_B T)$, where E, τ_0, and k_B are the activation energy, attempt relaxation time, and Boltzmann constant, respectively. However, τ_0 determined by the Arrhenius law ($\sim 10^{-17}$ Hz) is too small to be meaningful for the physical phenomena.[22,40] Thus, to reproduce the linear temperature dependence of τ, we apply the modified superparaelectric model (modified Arrhenius law)

$$\tau = \tau_0 \exp\left[\frac{E_0}{k_B}\left(\frac{1}{T} - \frac{1}{T_B}\right)\right], \tag{12}$$

in which the temperature dependence of E is roughly approximated to be $E_0(T_B - T)/T_B$, where E_0 is the energy barrier extrapolated to 0 K. This approximation represents that energy barrier separating the local states of dipole, which appears at T_B accompanying with the appearance of the dynamic PNRs, and then increases linearly on further cooling. To determine E_0 and τ_0, T_B is fixed to be 740 K for the three PZN-xPT samples. The fitted results by this model [Eq. (12)] are shown in Fig. 6 with solid lines, and the parameters are listed in Table I. The attempt frequency ($=1/2\pi\tau_0$) of the three crystals is $1.5 \sim 1.9 \times 10^{12}$ Hz, which is within the order of the typical Debye frequency range. This indicates that the model described in Eq. (12) is valid in the relaxor ferroelectrics. τ_0 decreases with the increasing PT concentration, while E_0 increases as shown in the inset of Fig. 6. This trend is consistent with our previous work on $(1-x)$ $Pb(Mg_{1/3}Nb_{2/3})O_3 - xPbTiO_3$ (PMN-xPT), which shows that

TABLE I. Fitted parameters of $\tau(T)$ to the modified superparaelectric model (modified Arrhenius law) for the PZN-xPT crystals. The fitted lines are described in Fig. 6.

x	E_0/k_B (K)	τ_0 (s)
0.07	3061	1.04405×10^{-13}
0.10	3406	9.68827×10^{-14}
0.12	4149	8.24161×10^{-14}

E_0 increases markedly with PT content increasing across the MPB.[22] The composition dependence of E_0 indicates that the energy barrier E becomes sensitive to the temperature with increasing x. As we suggested in Ref. 22, the comparatively large values of E_0 signify the specific mechanism of normal ferroelectric phase transition, in which abrupt growth of PNRs occurs at T_C rather than the parallel alignment of PNR's dipole moments due to ferroelectric-type interactions among PNRs.

Since the relaxor properties are closely connected with various dynamics with different length scales, a discussion regarding the length scale is important. The length scale L of the dynamics can be estimated from the present results using

$$L = S(\varphi) V \tau, \tag{13}$$

where $S(\varphi)$ is the shape parameter of the relaxation unit.[23,41] In this paper, we use $S(\varphi) = 1.0$ for simplicity, and only discuss L along the [100] direction in the paraelectric phase. L indicates the distance over which local relaxation interacts elastically, and a stress takes longer than τ to travel from a relaxation center to a distance greater than L. After this time τ, a new relaxation happens at the same relaxation center or nearby, and the process repeats. Thus, L captures the dynamic process of relaxation in a disordered system and denotes the maximal distance at which two relaxation centers interact. In the situation in which τ is determined by viscosity, L is called the *liquid elasticity length*.[42] In this study, τ and V are determined by the LA phonon along [100], so L is a characteristic length for the volume fluctuation along this direction.

The propagation length of the LA phonon per second is given by the phase velocity V, which is determined by our Brillouin scattering measurement through Eq. (1), where $\theta = 180^\circ$ and $\lambda_0 = 532 \times 10^{-9}$ m. The refractive index n is regarded as 2.7 for all the compositions and temperatures, and the change in n must be trivial compared with that in the parameters of the LA phonon.[5,43,44] The plots of V for the three PZN-xPT crystals are shown in Fig. 2.

Figure 7 plots the obtained values of L as a function of the temperature, showing that L is on the scale of nanometers.

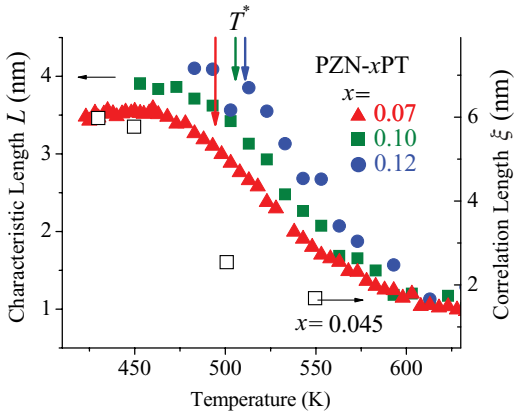

FIG. 7. (Color online) Temperature dependence of the characteristic length L along [100] of PZN-xPT crystals above T_C. The length scale L was determined from τ (Fig. 6) and V (Fig. 2) by using Eq. (13) with $S(\varphi) = 1.0$. The correlation length ξ along [100] determined by neutron diffuse scattering is also shown.[45]

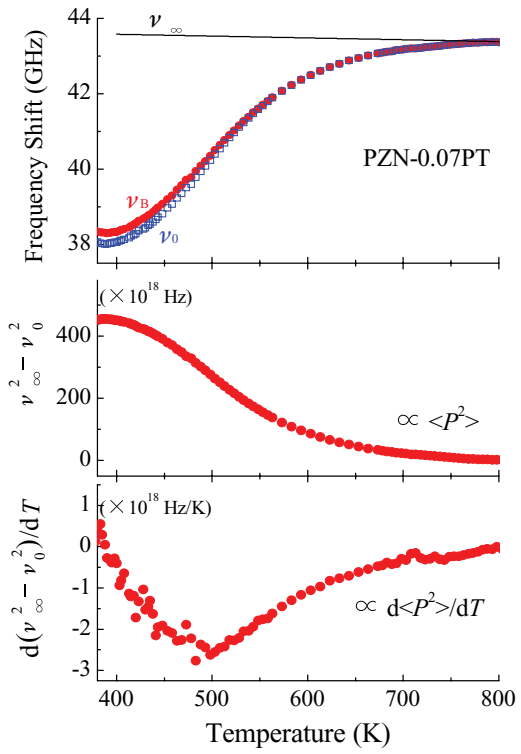

FIG. 8. (Color online) Temperature dependence of ν_B, ν_0, ν_∞ (upper), $\nu_\infty^2 - \nu_0^2 \propto \langle P^2 \rangle$ (middle), and $d(\nu_\infty^2 - \nu_0^2)/dT \propto d\langle P^2 \rangle/dT$ (lower) in PZN-0.07PT. The values of ν_0 were determined on the assumption of a single relaxation process at gigahertz range [Eq. (8)]. No other relaxations at lower frequency were taken into account.

As the temperature decreases, the change in L becomes larger; however, unlike the correlation length in normal ferroelectrics, L does not diverge when T approaches T_C. The correlation length determined by diffuse neutron scattering ξ is of the same order as L and depends on temperature in the same manner as L.[14,45] Therefore, we speculate that L may reflect the dynamic PNR. Because the larger dynamic PNRs transform into static below T^*, the dynamic PNRs cannot be larger than 3.5 nm below T^*. As a result, L does not grow below T^*. To confirm this interpretation of L, more data are required, along with a more refined discussion. However, this simple estimation of L can be accepted as a starting point for understanding the ferroelectric phase transition in relaxor ferroelectrics.

In Sec. III B, we discussed the fluctuation around ω_S Hz (∼40 GHz of Brillouin scattering frequency) because the imaginary part of the susceptibility is proportional to the spectral intensity of fluctuation.[46,47] However, the total fluctuation, $\langle P^2 \rangle$, is proportional to the real part of the susceptibility. On the assumption of one Debye-type dielectric relaxation around the gigahertz range [Eq. (8)], the Brillouin shift at the low-frequency limit, ν_0, can be calculated in a similar way as Eq. (11), and $\langle P^2 \rangle \propto c'(\infty) - c'(0) \propto \nu_\infty^2 - \nu_0^2$ can be determined. The determined values of ν_0 are shown in Fig. 8, with ν_∞ and ν_B. ν_0 shows similar temperature dependence to ν_B at high temperature and deviates from ν_B when approaching T_C, where the polarization fluctuates markedly. The quantities representing the total fluctuation are also shown in Fig. 8. The temperature dependence of $\nu_\infty^2 - \nu_0^2$ shows the growing process of polarization fluctuation upon cooling toward T_C. In the same way as shown in Fig. 4 in which the growth of fluctuation at ω_S Hz starts to be suppressed below T^*, $\langle P^2 \rangle \propto c'(\infty) - c'(0) \propto \nu_\infty^2 - \nu_0^2$ also shows an inflexion point, indicating that the growth of total fluctuation starts to be suppressed below T^*. The same trend is also found in PZN-0.10PT and PZN-0.12PT. Thus, it is concluded that inflexion point of the growing process in a paraelectric phase can be related to the characteristic properties of relaxor-based solid solutions.

IV. CONCLUSIONS

Brillouin scattering from PZN-xPT ($x = 0.07$, 0.10, and 0.12) crystals was measured, and the ferroelectric phase transition in relaxor ferroelectrics was discussed from the viewpoint of acoustic phonons. The acoustic anomaly was observed in all crystals in a wide temperature range and was described by a model involving piezoelectric coupling inside PNRs, even in the paraelectric phase. The anomaly at T_B indicates the appearance of fluctuating PNRs, and that at T^* represents the suppression of the growth rate of PNRs.

The relaxation time and the dynamic characteristic length scale were determined on the basis of the piezoelectric coupling inside PNRs. The relaxation time is of the order of 10^{-13} s, while the characteristic length is of the order of 10^{-9} m. Both of these do not grow markedly below T^*, which can be attributed to the suppression of growth of the polarization of PNRs. These results imply that static PNRs appear below T^*, and they generate random electric fields, which suppress the growth of polarization fluctuations. We believe that T^* is a distinguishing feature of relaxor ferroelectrics.

ACKNOWLEDGMENTS

We would like to thank Y. Akishige, M. Iwata, T.-H. Kim, J.-H. Ko, and K. Ohwada for stimulating discussions. This study was partly supported by the Electric Technology Research Foundation of Chugoku and the Grant-in-Aid for Young Scientists (B) program from MEXT, Japan. The work at Simon Fraser University was supported by the US Office of Naval Research (Grants No. N00014-06-1-0166 and No. N00014-11-1-0552) and the Natural Science and Engineering Research Council of Canada.

*Corresponding authors: tsukada@edu.shimane-u.ac.jp
†kojima@ims.tsukuba.ac.jp
‡zye@sfu.ca

[1] T. Tadaki, K. Otsuka, and K. Shimizu, Annu. Rev. Mater. Sci. **18**, 25 (1988).
[2] E. Dagotto, New J. Phys. **7**, 67 (2005).
[3] A. A. Bokov and Z.-G. Ye, J. Mater. Sci. **41**, 31 (2006).
[4] S.-E. Park and T. R. Shrout, J. Appl. Phys. **82**, 1804 (1997).
[5] G. Burns and B. A. Scott, Solid State Commun. **13**, 423 (1973).

[6]B. Dkhil, P. Gemeiner, A. Al-Barakaty, L. Bellaiche, E. Dul'kin, E. Mojaev, and M. Roth, Phys. Rev. B **80**, 064103 (2009).
[7]E. Dul'kin, M. Roth, P. E. Janolin, and B. Dkhil, Phys. Rev. B **73**, 012102 (2006).
[8]M. Roth, E. Mojaev, E. Dul'kin, P. Gemeiner, and B. Dkhil, Phys. Rev. Lett. **98**, 265701 (2007).
[9]D. Viehland, S. J. Jang, L. E. Cross, and M. Wuttig, J. Appl. Phys. **68**, 2916 (1990).
[10]M. El Marssi, R. Farhi, J. L. Dellis, M. D. Glinchuk, L. Seguin, and D. Viehland, J. Appl. Phys. **83**, 5371 (1998).
[11]J. Toulouse, F. Jiang, O. Svitelskiy, W. Chen, and Z.-G. Ye, Phys. Rev. B **72**, 184106 (2005).
[12]I.-K. Jeong, J. K. Lee, and R. H. Heffner, Appl. Phys. Lett. **92**, 172911 (2008).
[13]I.-K. Jeong, Phys. Rev. B **79**, 052101 (2009).
[14]G. Xu, G. Shirane, J. R. D. Copley, and P. M. Gehring, Phys. Rev. B **69**, 064112 (2004).
[15]G. Xu, P. M. Gehring, and G. Shirane, Phys. Rev. B **72**, 214106 (2005).
[16]S. Kamba, M. Kempa, V. Bovtun, J. Petzelt, K. Brinkman, and N. Setter, J. Phys.: Condens. Matter **17**, 3965 (2005).
[17]S. Tsukada, Y. Ike, J. Kano, T. Sekiya, Y. Shimojo, R. P. Wang, and S. Kojima, Appl. Phys. Lett. **89**, 212903 (2006).
[18]J.-H. Ko, D. H. Kim, S. Kojima, W. Z. Chen, and Z.-G. Ye, J. Appl. Phys. **100**, 066106 (2006).
[19]S. Tsukada, Y. Ike, J. Kano, T. Sekiya, Y. Shimojo, R. Wang, and S. Kojima, J. Phys. Soc. Jpn. **77**, 033707 (2008).
[20]S. Tsukada and S. Kojima, Phys. Rev. B **78**, 144106 (2008).
[21]K. Ohwada, K. Hirota, H. Terauchi, T. Fukuda, S. Tsutsui, A. Q. R. Baron, J. Mizuki, H. Ohwa, and N. Yasuda, Phys. Rev. B **77**, 094136 (2008).
[22]J.-H. Ko, D. H. Kim, S. Tsukada, S. Kojima, A. A. Bokov, and Z.-G. Ye, Phys. Rev. B **82**, 104110 (2010).
[23]S. Kojima and S. Tsukada, Ferroelectrics **405**, 32 (2010).
[24]W. Rehwald, Adv. Phys. **22**, 721 (1973).
[25]J. Kuwata, K. Uchino, and S. Nomura, Ferroelectrics **37**, 579 (1981).
[26]D. La-Orauttapong, B. Noheda, Z.-G. Ye, P. M. Gehring, J. Toulouse, D. E. Cox, and G. Shirane, Phys. Rev. B **65**, 144101 (2002).
[27]L. C. Lim, K. K. Rajan, and J. Jin, IEEE Trans. Ultrason. Ferroelectr. Freq. Control **54**, 2474 (2007).
[28]W. Chen and Z.-G. Ye, J. Mater. Sci. **36**, 4393 (2001).
[29]Z. Kutnjak, Ferroelectrics **400**, 214 (2010).
[30]Z. Li, M. Grimsditch, C. M. Foster, and S. K. Chan, J. Phys. Chem. Solids **57**, 1433 (1996).
[31]J.-H. Ko, S. Kojima, T. Y. Koo, J. H. Jung, C. J. Won, and N. J. Hur, Appl. Phys. Lett. **93**, 102905 (2008).
[32]J.-H. Ko, T. H. Kim, K. Roleder, D. Rytz, and S. Kojima, Phys. Rev. B **84**, 094123 (2011).
[33]S. Tsukada, Y. Hiraki, Y. Akishige, and S. Kojima, Phys. Rev. B **80**, 012102 (2009).
[34]P. M. Gehring, S. Wakimoto, Z.-G. Ye, and G. Shirane, Phys. Rev. Lett. **87**, 277601 (2001).
[35]C. Stock, L. Van Eijck, P. Fouquet, M. Maccarini, P. M. Gehring, G. Xu, H. Luo, X. Zhao, J. F. Li, and D. Viehland, Phys. Rev. B **81**, 144127 (2010).
[36]M. Matsuura, K. Hirota, P. M. Gehring, Z.-G. Ye, W. Chen, and G. Shirane, Phys. Rev. B **74**, 144107 (2006).
[37]K. Ohwada, J. Mizuki, K. Namikawa, M. Matsushita, S. Shimomura, H. Nakao, and K. Hirota, Phys. Rev. B **83**, 224115 (2011).
[38]V. V. Shvartsman and A. L. Kholkin, J. Appl. Phys. **101**, 064108 (2007).
[39]G. Burns and F. H. Dacol, Ferroelectrics **37**, 661 (1981).
[40]F. M. Jiang and S. Kojima, Phys. Rev. B **62**, 8572 (2000).
[41]S. Kojima, Jpn. J. Appl. Phys. **49**, 07HA01 (2010).
[42]K. Trachenko and V. V. Brazhkin, J. Phys.: Condens. Matter **20**, 075103 (2008).
[43]G. Burns and F. H. Dacol, Ferroelectrics **104**, 25 (1990).
[44]T. Sonehara, E. Tatsu, S. Saikan, and S. Ohno, J. Appl. Phys. **101**, 103507 (2007).
[45]D. La-Orauttapong, J. Toulouse, Z.-G. Ye, W. Chen, R. Erwin, and J. L. Roberston, Phys. Rev. B **67**, 134110 (2003).
[46]R. Kubo, M. Toda, and N. Hashitsume, *Statistical Physics II: Nonequilibrium Statistical Mechanics* (Springer, Heidelberg, 1991).
[47]L. D. Landau and E. M. Lifshtz, *Statistical Physics* (Butterworth-Heinemann, Oxford, 1980).